Implications of Cation Exchange on Clay Release and Colloid-Facilitated Transport in Porous Media

Scott A. Bradford* USDA–ARS
Hyunjung Kim Chonbuk National University

Column experiments were conducted to study chemical factors that influence the release of clay (kaolinite and quartz minerals) from saturated Ottawa sand of different sizes (710, 360, and 240 μm). A relatively minor enhancement of clay release occurred when the pH was increased (5.8 to 10) or the ionic strength (IS) was decreased to deionized (DI) water. In contrast, clay release was dramatically enhanced when monovalent Na^+ was exchanged for multivalent cations (e.g., Ca^{2+} and Mg^{2+}) on the clay and sand and then the solution IS was reduced to DI water. This solution chemistry sequence decreased the adhesive force acting on the clay as a result of an increase in the magnitude of the clay and sand zeta potential with cation exchange, and expansion of the double layer thickness with a decrease in IS to DI water. The amount of clay release was directly dependent on the Na^+ concentration of the exchanging solution and on the initial clay content of the sand (0.026–0.054% of the total mass). These results clearly demonstrated the importance of the order and magnitude of the solution chemistry sequence on clay release. Column results and scanning electron microscope (SEM) images also indicated that the clay was reversibly retained on the sand, despite predictions of irreversible interaction in the primary minimum. One plausible explanation is that adsorbed cations increased the separation distance between the clay–solid interfaces as a result of repulsive hydration forces. A cleaning procedure was subsequently developed to remove clay via cation exchange and IS reduction; SEM images demonstrated the effectiveness of this approach. The transport of Cu^{2+} was then shown to be dramatically enhanced by an order of magnitude in peak concentration by adsorption on clays that were released following cation exchange and IS reduction.

The migration of clay particles in porous media is an important process in soil genesis, erosion, and aquifer and petroleum reservoir production because it has a pronounced influence on the ability of porous media to transmit fluids and solutes (Khilar and Fogler, 1998; Mays and Hunt, 2005). Furthermore, the high surface area of clays that are mobile can facilitate the transport of many inorganic and organic contaminants that strongly adsorb to the solid phase (Grolimund et al., 1996; Kim et al., 2003; Simunek et al., 2006). Factors that influence clay release will also affect the fate of other colloidal contaminants such as pathogens, nanoparticles, and bacteria used in bioremediation operations (Bradford and Torkzaban, 2008). Hence, knowledge of the factors that influence clay release and transport is needed to efficiently manage a wide variety of environmental resources.

Clay release has commonly been assumed to be controlled by hydrodynamic and chemical perturbations. Increasing the velocity of water flow through porous media has been reported to enhance colloid release due to an increase of the hydrodynamic forces and torques that act on retained colloids (Bergendahl and Grasso, 1998, 1999, 2000). In contrast, chemical perturbations will influence the adhesive forces and torques that act to retain colloids. The solution ionic strength (IS) is a function of the ion molar concentration (M_i) and valence (Z_i) that is given as $0.5\Sigma(M_i Z_i^2)$. Enhanced colloid release is known to occur with a decrease in the IS due to an expansion of the double layer thickness and an increase in the magnitude of the surface potential (Israelachvili, 1992; Elimelech et al., 1995); both of these factors will lower the adhesive force. Increases in the solution pH will also enhance colloid release due to an increase in the electrostatic repulsion; that is, changes in the surface potentials may occur as a result of deprotonation of pH-dependent charge sites (Bohn et al., 1985; Ryan and Elimelech, 1996).

Ion exchange will influence the solution IS, double layer thickness, and surface potential due to their dependence on the ion valence. Divalent ions in solution will increase the solution IS and decrease the double layer thickness compared with similar concentrations of monovalent ions (Israelachvili, 1992; Elimelech et al., 1995). In addition, the magnitude of the colloid surface

---

J. Environ. Qual. 39:2040–2046 (2010)
doi:10.2134/jeq2010.0156
Published online 19 Aug. 2010.
Received 7 Apr. 2010.
*Corresponding author (scott.bradford@ars.usda.gov).
© ASA, CSSA, SSSA
5585 Guilford Rd., Madison, WI 53711 USA

S.A. Bradford, USDA–ARS, U.S. Salinity Lab., 450 W. Big Springs Rd., Riverside, CA 92507; H. Kim, Dep. of Mineral Resources and Energy Engineering, Chonbuk National Univ., 664-14 Duckjin, Jeonju, Jeonbuk 561-756, Republic of Korea. Assigned to Associate Editor Carl Bolster.

Abbreviations: DI, deionized; DLVO, Derjaguin–Landau–Verwey–Overbeek; IS, ionic strength; OD_{600}, optical density at 600 nm; PV, pore volume; SAR, sodium adsorption ratio; SEM, scanning electron microscope.

potential will be lower in the presence of adsorbed divalent than monovalent ions (Israelachvili, 1992; Elimelech et al., 1995; Khilar and Fogler, 1998). Increased clay retention and aggregation is therefore expected in the presence of divalent compared with monovalent ions as a result of the associated increase in the adhesive interaction (Israelachvili, 1992; Elimelech et al., 1995). Conversely, enhanced clay release and dispersion occurs in the presence of monovalent ions.

Much research has demonstrated the importance of ion exchange on changes in permeability in agricultural soils, aquifers, and petroleum reservoirs (Shainberg et al., 1981; Ayers and Westcot, 1989; Khilar and Fogler, 1998; Rinck-Pfeiffer et al., 2000; Suarez et al., 2006). Under these conditions, clay release and dispersion has been associated with significant decreases in the soil permeability as a result of clogging of the pore structure (Khilar and Fogler, 1998; Suarez et al., 2006). The sodium adsorption ratio (SAR) has frequently been used to characterize the clogging hazard of irrigation water based on the composition of sodium relative to calcium and magnesium (Ayers and Westcot, 1989). The SAR value reflects the preference of soils to adsorb calcium and magnesium ions over sodium ions and is correlated with the degree of sodium saturation on the exchange sites. Reduced soil permeability with higher SAR solutions has been well documented in the literature (Suarez et al., 2006).

Clogging of clays in porous media is known to be sensitive to the pore space geometry and size (McDowell-Boyer et al., 1986; Khilar and Fogler, 1998). In particular, high-permeability soils and aquifers with low amounts of clay are likely to be less susceptible to permeability changes as a result of ion exchange. It is possible that ion exchange will have a more pronounced influence in coarser-textured media due to the rapid filling of the cation exchange sites and subsequent transport of the released clays. Cation exchange will have important implications for colloid-facilitated transport of contaminants in these environments. Relatively little research has addressed the potential effects of ion exchange on clay release and colloid-facilitated transport in high-permeability soils (Roy and Dzombak, 1996; Grolimund et al., 1996; Grolimund and Borkovec, 2005, 2006). Roy and Dzombak (1996) observed large amounts of clay release from sand when Ca^{2+} was exchanged for Na^+ and then the eluting solution ionic strength was lower. These authors attributed this observation to strong selectivity of oxide surfaces for Ca^{2+} over Na^+. Colloid release and colloid-facilitated transport of Pb^{2+} has also been extensively studied in silt loam soil aggregates that contain a complex variety of colloid particles such as vermiculite, illite, kaolinite, muscovite, chlorite, and goethite (Grolimund et al., 1996; Grolimund and Borkovec, 2005, 2006). Colloid release, transport, and facilitated transport of $Pb^{2+}$was initiated by a reduction in the solution ionic strength when the exchange sites were dominated by Na^+ and then decreased abruptly when a Ca^{2+}–Na^+ exchange front appeared.

Although the above literature reports a strong sensitivity of clay release to the relative saturation of the medium with divalent cations, results were not explained in terms of differences in clay zeta potential or double layer thickness as a result of cation exchange. In addition, the extent of cation exchange will depend on the initial clay content as well as on the concentrations of the ions in solution and on the solid phase. This implies that the solution chemistry sequence and the initial clay content will play an important role in clay release, and this has not be fully demonstrated or appreciated in the literature.

The objective of this research was therefore to investigate the influence of cation exchange on clay release and colloid-facilitated transport in high-permeability sands with low amounts of clay. Special focus was placed on explaining results in terms of the solution chemistry sequence and its influence on measured zeta potentials of the sand and clay, calculated double layer thicknesses, and the mass balance of clay. A cleaning procedure was subsequently developed to remove clay from sand based on this information. The importance of solution chemistry sequence on clay release, transport, and facilitated transport of Cu^{2+} is also demonstrated in this work. Copper is a heavy metal contaminant that is found in fungicides, sewage sludge and animal wastes, and wastes from a variety of industrial operations (e.g., timber preservation and mining operations).

Materials and Methods

Ottawa sands are natural aquifer material reported to consist of 99.8% SiO_2 (quartz) and trace amounts of metal oxides. Three different size fractions of Ottawa sand were utilized in the experiments discussed below with median grain sizes of 710, 360, and 240 μm and with coefficients of uniformity equal to 1.21, 1.88, and 3.06, respectively. Although these sands are relatively uniform, they still contain small amounts of clay. The amount and characteristics of this clay, and factors that influence their release will be discussed as part of this research.

Aqueous solutions of various IS and pH were used in experiments. Solutions consisted of deionized (DI) water with its unadjusted pH = 5.8 or adjusted to a pH = 10 using 1.7 mM of Na_2CO_3 and 1.7 mM of $NaHCO_3$. Various IS levels from 1 to 106 mM were achieved by adding NaCl or $CaCl_2$.

Glass chromatography columns (15 cm long and 4.8 cm i.d.) were used in clay release experiments. The columns were wet packed with a given size of Ottawa sand. Additional information on the column protocols were reported by Bradford et al. (2002). Various pulses of aqueous solutions at selected chemistries were pumped upward through the vertically oriented columns at a steady flow rate. The sequence and composition of the aqueous solutions for a given experiment was selected to test specific hypotheses with regard to clay release or to demonstrate potential applications. Table 1 provides values of the aqueous solution chemistry sequence and duration (T_o) in terms of pore volumes (PV) for each experiment. Other column properties were relatively constant and included the porosity (ε = 0.33–0.36), the column length (L_c = 12.8–13.0 cm), and the Darcy velocity (q = 0.26 to 0.28 cm min^{-1}). Effluent samples were collected using a fraction collector (RTRV II, Isco Inc, Lincoln, NE) and analyzed for clay concentration using a spectrophotometer (Unico UV-2000, United Products & Instruments, Dayton, NJ) at an optical density at 600 nm (OD_{600}). A linear correlation was established between OD_{600} and the clay mass that was determined after drying effluent samples. This correlation was verified to be independent of the solution chemistry for our experimental conditions. Select effluent samples were also analyzed for

Table 1. The injection solution chemistry sequence for each experimental system. The pulse duration (T_0) in terms of pore volumes is given in parentheses.

Fig. no.	Index	Injection solution chemistry sequence (T_0)†
Figure 1	710 μm	DI→6 mM NaCl (2.0)→106 mM NaCl (2.3)→DI→6 mM NaCl (3.3)→106 mM NaCl (1.3)→FI‡→106 mM NaCl (1.0)→DI→FI§→DI
	360 μm	DI→6 mM NaCl (1.9)→106 mM NaCl (2.1)→DI→6 mM NaCl (3.0)→106 mM NaCl (1.2)→FI‡→106 mM NaCl (0.9)→DI→FI§→DI
	240 μm	DI→6 mM NaCl (2.0)→106 mM NaCl (2.2)→DI→6 mM NaCl (3.2)→106 mM NaCl (1.2)→FI‡→106 mM NaCl (1.0)→DI→FI§→DI
Figure 3	1 mM NaCl	DI→1 mM NaCl (3.8)→DI→100 mM NaCl (3.3)→DI
Figure 4a	0.1 mM NaCl	DI→0.1 mM NaCl (3.1)→DI→100 mM NaCl (2.5)→DI
	1 mM NaCl	DI→1 mM NaCl (3.8)→DI→100 mM NaCl (3.3)→DI
	10 mM NaCl	DI→10 mM NaCl (3.0)→DI→100 mM NaCl (2.4)→DI
	100 mM NaCl	DI→100 mM NaCl (3.2)→DI→100 mM NaCl (2.6)→DI
Figure 4b	100 mM $CaCl_2$	DI→100 mM $CaCl_2$ (3.0)→DI→100 mM NaCl (4.7)→DI
Figure 6	100 mM NaCl+2.5 mg L^{-1} Cu^{2+}	100 mM NaCl+2.5 mg L^{-1} Cu^{2+} (3.4)→100 mM NaCl (1.7)→DI

† FI, flow interruption; DI, deionized water.

‡ FI duration was 15.8 h.

§ FI duration was 0.5 h.

conductivity and pH (Oakton pH/CON 510 Benchtop Meter, Oakton Instruments, Vernon Hills, IL) and for cations using an inductively coupled plasma atomic emission spectrograph (Optima 3000, Dual View, PerkinElmer, Covina, CA).

Samples of the clay suspension from these release experiments were analyzed to characterize specific chemical and physical properties of the clay. Subsamples of the clay were saturated with Mg^{2+} and K^+ and prepared as paste mounts (Theisen and Harward, 1962) for X-ray diffraction at room temperature. Analyses were performed on a D-500 X-ray diffractometer (Siemens, Iselin, NJ) with a graphite crystal monochromator, and using CuKα radiation (40 kV and 30 mA). The zeta potential of selected clay suspensions was calculated from experimentally measured electrophoretic mobilities at 25°C using a ZetaPALS instrument (Brookhaven Instruments Corporation, Holtsville, NY) and the Smoluchowski equation; that is, the zeta potential (units of mV) equals 12.8 times the electrophoretic mobility (units of 10^{-8} m^2 V^{-1} s^{-1}). The particle size distribution of selected clay suspensions were measured with a Horiba LA 930 laser scattering particle size distribution analyzer (Horiba Instruments, Irvine, CA). A scanning electron microscope (XL30-FEG, Philips, Eindhoven, The Netherlands) was used to examine the morphology of clay deposits on Ottawa sand samples.

The total interaction energy of the clay particles on approach to a quartz surface under the various solution chemistries was calculated using Derjaguin–Landau–Verwey–Overbeek (DLVO) theory and a sphere-plate assumption (Derjaguin and Landau, 1941; Verwey and Overbeek, 1948). The retarded London–van der Waals attractive interaction force was determined from the expression of Gregory (1981) utilizing a value of 3.2E-20 J for the Hamaker constant (Khilar et al., 1990). Electrostatic double layer interactions were quantified using the expression of Hogg et al. (1966) using zeta potentials in place of surface potentials. The zeta potential of Ottawa (quartz) sand crushed to a powder was measured under the various solution chemistry conditions using the ZetaPALS instrument.

An additional clay release experiment was conducted in the presence of Cu^{2+} to investigate the potential for facilitated transport by the clay in 360-μm Ottawa sand. The input concentration (C_i) of Cu^{2+} used in this experiment was 2.5 mg L^{-1}; a stock solution of 1000 mg L^{-1} of $Cu(NO_3)_2$ (Aldrich Co., St. Louis, MO) was diluted for this purpose. The solution chemistry sequence for this experiment is provided in Table 1, and similar protocols were used as for the other clay release experiments. The concentration of Cu^{2+} in the effluent solution and adsorbed to clay was determined using the method of Lee and Choi (2001). In brief, 0.5 mL of 0.1% ammonium pyrrolidinedithiocarbamate and 1 mL of 1% Tween 80 (ICI Americas, Inc., Wilmington, DE) were added to 5 mL of the effluent sample. Then 3.5 mL of phosphate buffer was added to this solution. After equilibrating for 20 min, the absorbance of the effluent sample was measured using the spectrophotometer at a wavelength of 445 nm. The effluent sample was subsequently centrifuged at 5311 *g* for 30 min, and the supernatant was again analyzed with the spectrophotometer at 445 nm. Separate linear calibration curves were established between the ultraviolet absorbance and Cu^{2+} concentration in solution and in the presence of clays (the calibration was independent of the clay concentration). The detection limit of Cu^{2+} using this method has been reported to be 0.0393 mg L^{-1} (Lee and Choi, 2001).

Results and Discussion

The first series of experiments shown in Fig. 1 was designed to investigate the influence of transients in solution IS and pH on clay release for the 710-, 360-, and 240-μm sands. The solution chemistry sequence consisted of the following steps: (A) DI water at pH = 5.8, (B) 1 mM NaCl in pH = 10 solution (total IS = 6 mM), and (C) 100 mM NaCl in pH = 10 solution (total IS = 106 mM). This same solution chemistry cycle was repeated during Steps D, E, and F followed by an additional pulse of DI water at pH = 5.8 during Step G. The duration of each aqueous solution pulse is given in Table 1, and the steady-state Darcy velocity was maintained at 0.27 cm min^{-1}. The clay fraction was determined by X-ray diffraction to consist entirely of kaolinite and quartz.

Several interesting observations can be made about the information presented in Fig. 1. First, even though the same

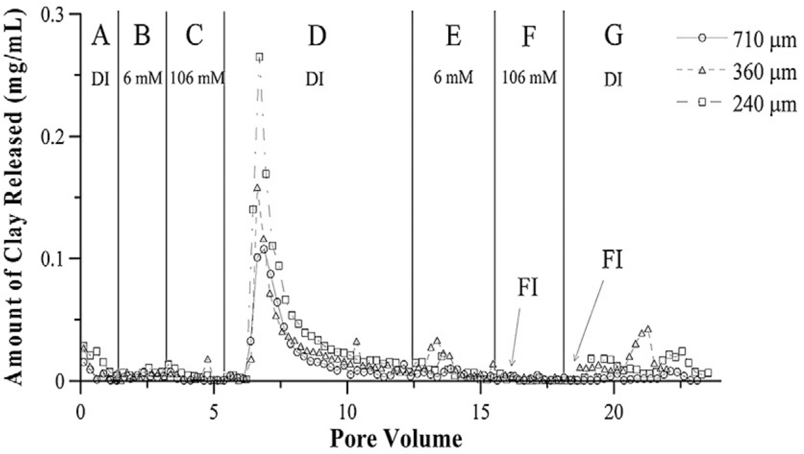

Fig. 1. The effluent concentration of clay released from 710-, 360-, and 240-µm Ottawa sands as a function of pore volume. The solution chemistry sequence consisted of the following steps: (A) deionized (DI) water at pH = 5.8; (B) 1 mM NaCl in pH = 10 solution (total ionic strength [IS] = 6 mM); and (C) 100 mM NaCl in pH = 10 solution (total IS = 106 mM). This same solution chemistry cycle was repeated during Steps D, E, and F followed by an additional pulse of DI water at pH = 5.8 during Step G. The duration of each aqueous solution pulse is given in Table 1, and the steady-state Darcy velocity was maintained at 0.27 cm min^{-1}. Periods of flow interruption are denoted with FI.

solution chemistry sequence was followed, very different amounts of clay were released from the three sands. The total mass of released clay increased with decreasing sand size (17.2, 27.5, and 35.4 mg of clay was released for the 710-, 360-, and 240-µm sand, respectively). This difference was largely due to the initial clay content of the sands, as is discussed below. The second observation is that the solution chemistry order had a profound influence on the amount of clay that was released. Limited amounts of clay release occurred during Step A (DI water) as a result of expansion of the double layer thickness and elimination of the secondary minimum. Steps B and E were associated with an increase in the solution pH from 5.8 (Steps A and D) to 10 (Steps B and E) and a slight increase in the IS (DI to IS = 6 mM), and the low values of clay in the effluent suggest that changes in pH had a relatively minor influence on clay release. Clay release is expected to decrease with an increase in IS due to compression of the double layer and an associated increase in the adhesive force. However, little or no decrease in clay release was observed when the IS was increased from 6 mM (Steps B and E) to 106 mM (Steps C and F). A tremendous increase in the amount of clay release occurred during Step D when the solution was switched to DI at pH = 5.8. In contrast, much lower amounts of clay release occurred for this same solution chemistry during Steps A and G (DI water). We hypothesize that differences in clay release during Steps A, D, and G (DI water) can be attributed to cation exchange during Steps C and F (100 mM NaCl with pH = 10), and depletion of clays from the sand surface over the course of experiment. Specifically, we postulate that Na^+ replaces multivalent cations, such as Ca^{2+} or Mg^{2+}, on the clay surface during Steps C and F (100 mM NaCl with pH = 10). This type of ion exchange would decrease the adhesive force acting on the clay, due to an increase in the double layer thickness and the magnitude of the clay zeta potential (Israelachvili, 1992; Elimelech et al., 1995; Khilar and Fogler, 1998). Upon reduction of the IS during Steps D and G (DI water), clay is released due to the further reduction in the adhesive force.

To test this hypothesis, the zeta potential of released clay during Steps A, D, and G (DI water) was measured. Mean and standard deviation values of the clay zeta potentials are presented in Fig. 2 for the various sands during Steps A, D, and G. Before addition of Na^+, the mean value of the zeta potential of released clay during Step A is approximately −26.6 mV. After addition of Na^+ during Steps C and F (100 mM NaCl with pH = 10), the mean value of the zeta potential of released clay during Steps D and G (DI water) was decreased to approximately −53.8 mV. This observation is consistent with results of exchange of monovalent and divalent cations (Khilar and Fogler, 1998). It should also be mentioned that the median clay size in the effluent during Steps A and D was 2.39 and 0.76 µm, respectively. The applied hydrodynamic torque that acts on spherical colloids at a small separation distance from a solid surface is proportional to the cube of the colloid radius (Goldman et al., 1967), and it is predicted to be approximately 31 times larger for 2.39-µm particles compared with 0.76-µm particles. This observed decrease in clay size after exposure to 100 mM NaCl is therefore likely to be a result of differences in the applied hydrodynamic torque with particle size and indicates that it was more difficult to remove the smaller-sized clay particles.

Five clay release experiments were conducted to further test and understand the cation exchange hypothesis. These experiments utilized 360-µm sand and aqueous solutions at pH = 5.8. The solution chemistry sequence for the first column consisted of the following steps: (A) DI water; (B) 0.1 mM NaCl; (C) DI water; (D) 100 mM NaCl; and (E) DI water. This same solution chemistry cycle was repeated for columns 2, 3, 4, and

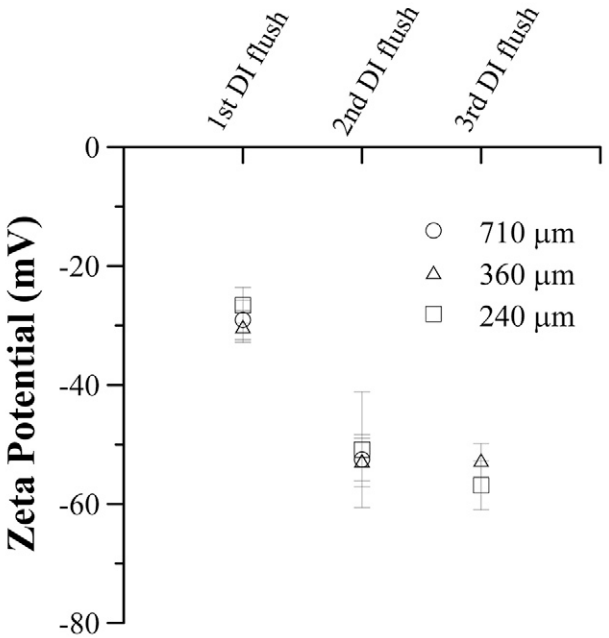

Fig. 2. Measured values of zeta potential for clay released during Steps A, D, and G shown in Fig. 1. Mean and standard deviation values of the clay zeta potentials are presented. DI, deionized water.

5 but with 1 mM NaCl, 10 mM NaCl, 100 mM NaCl, and 100 mM $CaCl_2$, respectively, added during Step B. The duration of each aqueous solution pulse is given in Table 1, and the Darcy velocity was 0.27 cm min^{-1}. Values of the zeta potential and double layer thickness (Debye length) for the clay and sand under these various solution chemistry conditions are provided in Table 2.

Table 2. The average and standard deviation (in parentheses) of measured zeta potentials for clay particles (ζ_c) and crushed Ottawa sand (ζ_s) in the indicated solution chemistries, and the calculated Debye length.

Solution chemistry	ζ_s	ζ_c	Debye length
	——— mV ———		nm
Deionized water	−49.3 (3.4)	−39.6 (1.9)	960†
0.1 mM NaCl	−75.5 (4.8)	−56.7 (1.8)	30.5
1 mM NaCl	−73.6 (2.0)	−71.7 (4.4)	9.6
10 mM NaCl	−64.8 (3.2)	−66.9 (3.6)	3.1
100 mM NaCl	−57.3 (9.3)	−38.6 (8.9)	1.0
100 mM $CaCl_2$	−38.6 (3.5)	−10.6 (16.5)	0.6

† Taken from Gregory (2006).

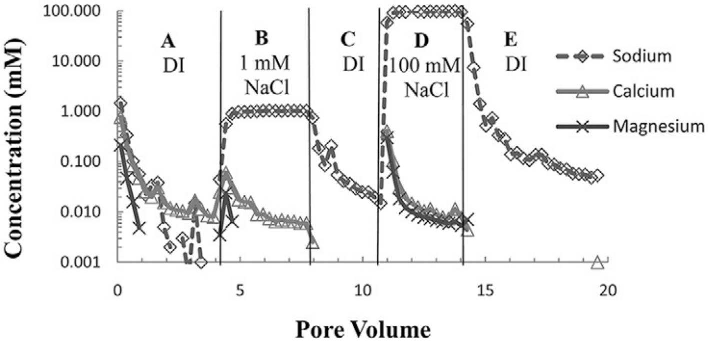

Fig. 3. A semi-log plot of the effluent concentrations of Na^+, Ca^{2+}, and Mg^{2+} (mM) as a function of solution pore volumes that were passed through a column packed with 360-μm Ottawa sand. The influent solution chemistry sequence (pH = 5.8) consisted of the following steps: (A) deionized (DI) water; (B) 1 mM NaCl; (C) DI water; (D) 100 mM NaCl; and (E) DI water. The duration of each aqueous solution pulse is given in Table 1, and the Darcy velocity was 0.27 cm min^{-1}.

Figure 3 presents a semi-log plot of the effluent concentrations of Na^+, Ca^{2+}, and Mg^{2+} (mM) as a function of solution pore volumes that were passed through column 2. Effluent concentrations for these cations all decreased rapidly to low levels when DI water was added during Steps A, C, and E. Breakthrough of Na^+ added during Steps B and D resulted in a corresponding initial increase in the effluent concentrations of Ca^{2+} and Mg^{2+} that was proportional to the influent Na^+ level as a result of exchange on the sand and clay. However, continued addition of Na^+ at a given concentration was associated with a rapid decrease in the Ca^{2+} and Mg^{2+} concentrations, presumably due to depletion of Ca^{2+} and Mg^{2+} on readily accessible clay and sand surfaces.

Figure 4 presents the results from the clay release experiments outlined above. Exchange of Na^+ for Ca^{2+} and Mg^{2+} during Steps B and D (Fig. 3) produced an increase in the magnitude of the zeta potential of the clay and sand (Fig. 2, Table 2). However, this change in clay zeta potential did not result in an increase in the amount of clay released during Steps B and D. Conversely, the amount of clay released during Step C (DI water) was directly proportional to the amount of Na^+ added during Step B (Fig. 4a). Note especially that no clay release occurred during Step C in column 5, which was flushed with 100 mM $CaCl_2$ solution during Step B (Fig. 4b). Clay release therefore occurred as a result of both an increase in the magnitude of the clay zeta potential (cation exchange) during Steps B and D and an expansion of the double layer thickness (Table 2) with the IS reduction in Steps C and E.

The clay release that occurred during Step C apparently increased the accessibility of adsorbed Ca^{2+} and Mg^{2+} on remaining clay and sand surfaces. After adding 100 mM NaCl solution to all of the columns during Step D, Ca^{2+} and Mg^{2+}were again released (Fig. 3) as a result of exchanged with the Na^+. The amount of clay released during Step E was inversely proportion to the amount of Na^+ added during Step B. This can be attributed to the different amount of clay on the sand during step D as a result of clay removal during step C. Hence, results from Fig. 2, 3, and 4 provide convincing evidence that the combination of cation exchange, solution chemistry sequence, and initial clay content controlled the clay release in these experiments.

The DLVO interaction energy for the clay with quartz sand was subsequently determined using information presented in Table 2. Clay was predicted to be retained in the primary energy minimum in 100 mM NaCl and $CaCl_2$ solutions: that is, no energy barrier to clay attachment (favorable attachment conditions). Colloid interaction in the primary minimum is frequently assumed to be irreversible and therefore insensitive to changes in the solution IS or composition (Ryan and Elimelech, 1996). Results shown in Fig. 1 and 4, however, clearly demonstrate that the clay was reversibly retained in the sand. One plausible explanation derives from the presence of non-DLVO forces (e.g., Born repulsion, hydration forces, and steric interactions) between the clay–sand interfaces that limits their separation distance (Elimelech et al., 1995; Israelachvili, 1992). In particular, repulsive hydration forces have been reported to act between silica, mica, and clay surfaces at distances less than about 3 to 4 nm when the salt concentration is above a threshold value that is specific to the electrolyte (Israelachvili, 1992). These forces arise from the energy needed to dehydrate bound cations and increase with the hydrated radius (Mg^{2+}, Ca^{2+}, and Na^+ are 0.43, 0.41, and 0.36 nm, respectively) of the cation (Elimelech et al., 1995; Israelachvili, 1992).

Several potential applications of clay release by cation exchange and IS reduction are discussed below. Clay removal from sand surfaces may be desirable to decrease the reactivity of these surfaces to specific solutes and/or colloids, to collect samples of clay for analyses, to remediate contaminants associated with the clay fraction, and to enhance the permeability of the sands. Using the information presented in Fig. 1 to 4, the following cleaning protocol was developed to remove clays from sand: (i) a 400-g sample of sand was placed on a sieve and flushed with DI water, and (ii) the sieve and sand was immersed into 500 mM NaCl solution for 1 h and then flushed with DI water. This step was repeated until the OD_{600} of the effluent DI water achieved an acceptable level. The number of times that Step (ii) was repeated depended on the sand size and the initial clay content. As a final cleaning step, the sand was added to excess DI water and sonicated for 1 h followed by an additional DI water rinse. The efflu-

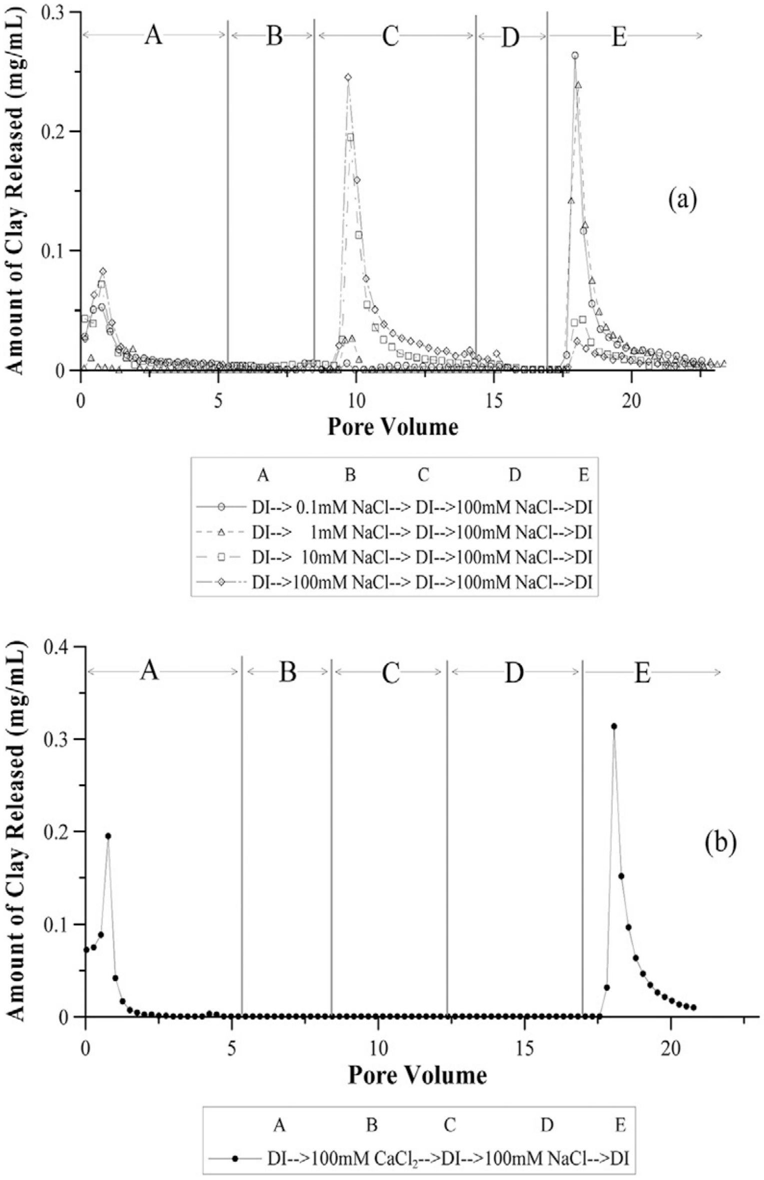

Fig. 4. The effluent concentration of clay released from 360-μm Ottawa sands as a function of pore volumes when the solution pH = 5.8. The solution chemistry sequence for the first column consisted of the following steps: (A) deionized (DI) water; (B) 0.1 mM NaCl; (C) DI water; (D) 100 mM NaCl; and (E) DI water. This same solution chemistry cycle was repeated for columns 2, 3, 4, and 5 but with 1 mM NaCl, 10 mM NaCl, 100 mM NaCl, and 100 mM CaCl$_2$ added during Step B, respectively. The duration of each aqueous solution pulse is given in Table 1, and the Darcy velocity was 0.27 cm min^{-1}.

ent from this cleaning protocol was collected and concentrated by centrifugation for analyses as needed. This cleaning protocol was used to collect clay samples for mineralogy analyses and to determine the initial clay content of our sands. The initial clay content, determined by weighing the dry pellet, was found to be 102.7, 135.2, and 214.8 mg for the 710-, 360-, and 240-μm sand, respectively. These sands contained a miniscule percentage of clay (0.026–0.054%), and only 16.7, 20.3, and 16.5% of this initial clay was recovered from the 710-, 360-, and 240-μm sand, respectively, during the experiment shown in Fig. 1.

The efficiency of the cleaning protocol was assessed by examining samples of 360-μm Ottawa sand with a SEM before and after treatment. Images are shown in Fig. 5. An abundance of clays was observed near macroscopic surface roughness locations before implementing the cleaning protocol. In contrast, these same locations were almost completely devoid of clays after cleaning, indicating that the clays have been efficiently removed by the combination of cation exchange and IS reduction. This observation implies that the clays were reversibly retained on the solid surface and that non-DLVO forces likely played a role in their release.

The potential influence of clay release from 360-μm Ottawa sand on Cu^{2+} transport was subsequently investigated. The following solution chemistry sequence was followed: (A) 100 mM NaCl+2.5 mg L^{-1} Cu^{2+}, (B) 100 mM NaCl, and (C) DI water. The duration of each aqueous solution pulse is provided in Table 1, and the Darcy velocity was 0.26 cm min^{-1}. Figure 6 presents the corresponding effluent concentrations of clay, free Cu^{2+} in solution, and Cu^{2+} adsorbed to clay as a function of PV. The concentration of free Cu^{2+} in the effluent was always low ($C/C_i < 0.05$). In contrast, concentrations of adsorbed Cu^{2+} were more than an order of magnitude higher and reach a peak value of approximately $C/C_i = 0.6$ when clay release occurred during Step C (DI water). The adsorbed concentration of Cu^{2+} coincided with the clay concentration and subsequently decreased with diminished clay release during Step C. These results clearly demonstrate that clay release as a result of cation exchange and IS reduction can dramatically facilitate the transport of Cu^{2+} in the environment.

Summary and Conclusions

Results presented in this work indicate that the initial clay content and the order and magnitude of the solution chemistry sequence can play a significant role in clay release from sands. In particular, exchange of Na^{+} for multivalent cations (such as Ca^{2+} and Mg^{2+}) followed by IS reduction has been demonstrated to enhance clay release due to an increase in the double layer thickness and the magnitude of the clay zeta potential. Furthermore, clay was found to be reversibly retained on the sand surface, despite DLVO predictions to the contrary (presumably due to non-DLVO forces). Potential applications of cation exchange were demonstrated for cleaning of sands. Clay was also demonstrated to facilitate Cu^{2+} transport as a result of cation exchange and IS reduction. Other potential applications of cation exchange and IS reduction include the removal of pathogens, other biocolloids, and biofilms from solid surfaces. These topics warrant additional research attention.

Acknowledgments

This research was supported by the 206 Manure and Byproduct Utilization Project of the USDA-ARS, and by a grant from NRI (NRI 2006-02541). Mention of trade names and company names in this manuscript does not imply any endorsement or preferential treatment by the USDA. We would also like to acknowledge the help of Lorena Altamirano in conducting some of the clay release experiments, Dr. Chong Hyun Chang in taking the SEM photos, Judith Turk and Dr. Robert Graham for performing the clay mineralogy analyses, and Dr. Sabine Goldberg for many helpful discussions.

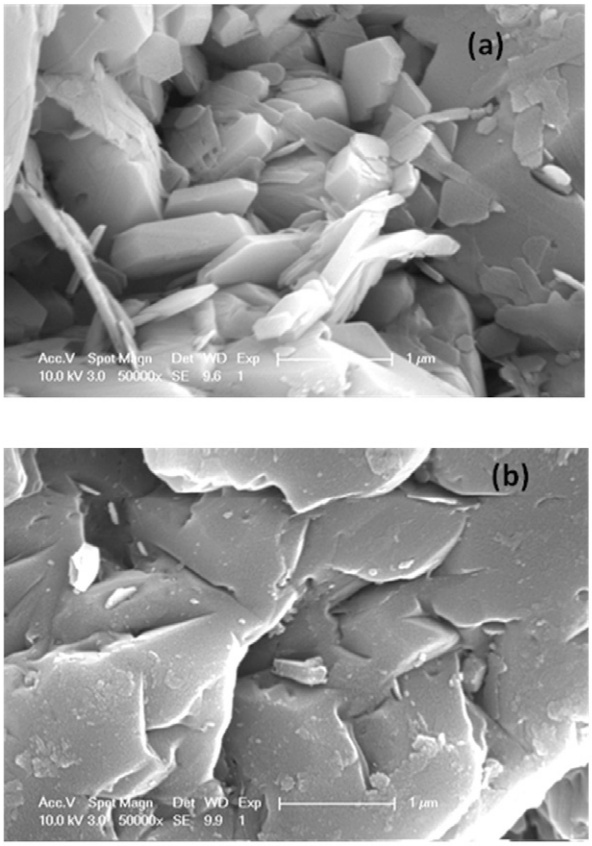

Fig. 5. Scanning electron microscope images of 360-μm Ottawa sand (a) before and (b) after using the cation exchange and ionic strength reduction cleaning protocol discussed in the text.

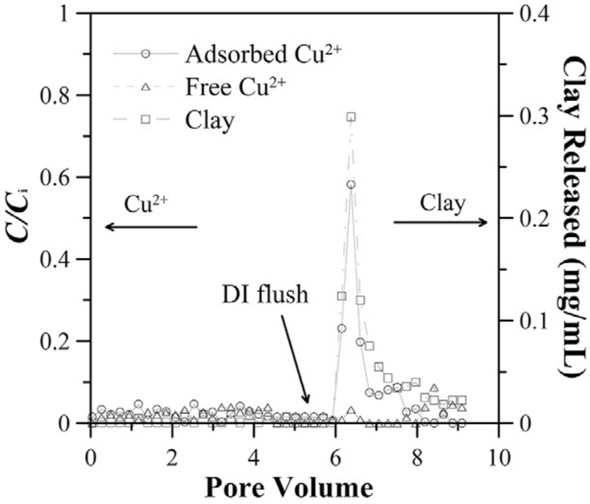

Fig. 6. Effluent concentrations (*C*) of clay and normalized concentration (C/C_i) of free Cu^{2+} in solution and Cu^{2+} adsorbed to clay as a function of pore volumes flushed through 360-μm Ottawa sand. The following solution chemistry sequence was followed: (A) 100 mM NaCl+2.5 mg L^{-1} Cu^{2+}; (B) 100 mM NaCl; and (C) deionized (DI) water. The duration of each aqueous solution pulse is provided in Table 1, and the Darcy velocity was 0.27 cm min^{-1}. The value of the influent Cu^{2+} concentration (C_i) was 2.5 mg L^{-1}.

References

Ayers, R.S., and D.W. Westcot. 1989. Water quality for agriculture. FAO Irrigation and Drainage Paper 29 Rev. 1. FAO, Rome.

Bergendahl, J., and D. Grasso. 1998. Colloid generation during batch leaching tests: Mechanics of disaggregation. Colloid Surf. A Physicochem. Eng. Aspects 135:193–205.

Bergendahl, J., and D. Grasso. 1999. Prediction of colloid detachment in a model porous media: Thermodynamics. AIChE J. 45:475–484.

Bergendahl, J., and D. Grasso. 2000. Prediction of colloid detachment in a model porous media: Hydrodynamics. Chem. Eng. Sci. 55:1523–1532.

Bohn, H.L., B.L. McNeal, and G.A. O'Connor. 1985. Soil chemistry. 2nd ed. John Wiley & Sons, New York.

Bradford, S.A., and S. Torkzaban. 2008. Colloid transport and retention in unsaturated porous media: A review of interface, collector, and pore scale processes and models. Vadose Zone J. 7:667–681.

Bradford, S.A., S.R. Yates, M. Bettahar, and J. Simunek. 2002. Physical factors affecting the transport and fate of colloids in saturated porous media. Water Resour. Res. 38:1327, doi:10.1029/2002WR001340.

Derjaguin, B.V., and L.D. Landau. 1941. Theory of the stability of strongly charged lyophobic sols and of the adhesion of strongly charged particles in solutions of electrolytes. Acta Phys. Chim. URSS 14:733–762.

Elimelech, M., J. Gregory, X. Jia, and R.A. Williams. 1995. Particle deposition & aggregation measurement, modeling, and simulation. Butterworth-Heinemann, Woburn, MA.

Goldman, A.J., R.G. Cox, and H. Brenner. 1967. Slow viscous motion of a sphere parallel to a plane wall: I. motion through a quiescent fluid. Chem. Eng. Sci. 22:637–651.

Gregory, J. 1981. Approximate expression for retarded van der Waals interaction. J. Colloid Interface Sci. 83:138–145.

Gregory, J. 2006. Particles in water: Properties and processes. CRC Press, Taylor & Francis Group, London.

Grolimund, D., and M. Borkovec. 2005. Colloid-facilitated transport of strongly sorbing contaminants in natural porous media: Mathematical modeling and laboratory column experiments. Environ. Sci. Technol. 39:6378–6386.

Grolimund, D., and M. Borkovec. 2006. Release of colloidal particles in natural porous media by monovalent and divalent cations. J. Contam. Hydrol. 87:155–175.

Grolimund, D., M. Borkovec, K. Barmettler, and H. Sticher. 1996. Colloid-facilitated transport of strongly sorbing contaminants in natural porous media: A laboratory column study. Environ. Sci. Technol. 30:3118–3123.

Hogg, R., T.W. Healy, and D.W. Fuerstenau. 1966. Mutual coagulation of colloidal dispersions. Trans. Faraday Soc. 62:1638–1651.

Israelachvili, J.N. 1992. Intermolecular and surface forces. 2nd ed. Academic Press, London.

Khilar, K.C., and H.S. Fogler. 1998. Migration of fines in porous media. Kluwer Academic, Dordrecht, the Netherlands.

Khilar, K.C., R.N. Vaidya, and H.S. Fogler. 1990. Colloidally-induced fines release in porous media. J. Petrol. Sci. Eng. 4:213–221.

Kim, S.B., M.Y. Corapcioglu, and D.J. Kim. 2003. Effect of dissolved organic matter and bacteria on contaminant transport in riverbank filtration. J. Contam. Hydrol. 66:1–23.

Lee, S.K., and H.-S. Choi. 2001. Spectrophotometric determination of cadmium and copper with ammonium pyrrolidinedithiocarbamate in nonionic Tween 80 micellar media. Bull. Korean Chem. Soc. 22:463–466.

Mays, D.C., and J.R. Hunt. 2005. Hydrodynamic aspects of particle clogging in porous media. Environ. Sci. Technol. 39:577–584.

McDowell-Boyer, L.M., J.R. Hunt, and N. Sitar. 1986. Particle transport through porous media. Water Resour. Res. 22:1901–1921.

Rinck-Pfeiffer, S., S. Ragusa, P. Sztajnbok, and T. Vandevelde. 2000. Interrelationships between biological, chemical, and physical processes as an analog to clogging in aquifer storage and recovery (ASR) wells. Water Res. 34:2110–2118.

Roy, S.B., and D. Dzombak. 1996. Colloid release and transport processes in natural and model porous media. Colloid Surf. A Physicochem. Eng. Aspects 107:245–262.

Ryan, J.N., and M. Elimelech. 1996. Colloid mobilization and transport in groundwater. Colloid Surf. A Physicochem. Eng. Aspects 107:1–56.

Shainberg, I., J.D. Rhoades, and R.J. Prather. 1981. Effect of low electrolyte concentration on clay dispersion and hydraulic conductivity of a sodic soil. Soil Sci. Soc. Am. J. 45:273–277.

Simunek, J., C. He, L. Pang, and S.A. Bradford. 2006. Colloid-facilitated transport in variably-saturated porous media: Numerical model and experimental verification. Vadose Zone J. 5:1035–1047.

Suarez, D.L., J.D. Wood, and S.M. Lesch. 2006. Effect of SAR on water infiltration under a sequential rain-irrigation management system. Agric. Water Manage. 86:150–164.

Theisen, A.A., and M.E. Harward. 1962. A paste method for preparation of slides for clay mineral identification by x-ray diffraction. Soil Sci. Soc. Am. Proc. 26:90–91.

Verwey, E.J.W., and J.Th.G. Overbeek. 1948. Theory of the stability of lyophobic colloids. Elsevier, Amsterdam, the Netherlands.